IEEE Photonics Journal
An IEEE Photonics Society Publication

Open Access

Performance Analysis of Free-Space Optical Communication Systems With Multiuser Diversity Over Atmospheric Turbulence Channels

Volume 6, Number 2, April 2014

Liang Yang
Xiqi Gao, Senior Member, IEEE
Mohamed-Slim Alouini, Fellow, IEEE

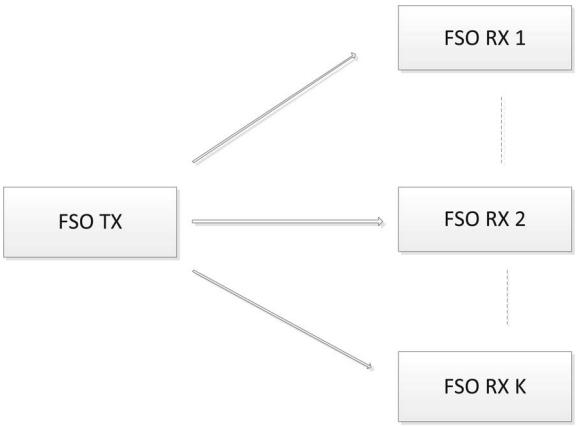

DOI: 10.1109/JPHOT.2014.2311446
1943-0655 © 2014 IEEE

IEEE photonics SOCIETY

IEEE

Performance Analysis of Free-Space Optical Communication Systems With Multiuser Diversity Over Atmospheric Turbulence Channels

Liang Yang,[1,2] **Xiqi Gao,**[2] ***Senior Member, IEEE*, and Mohamed-Slim Alouini,**[3] ***Fellow, IEEE***

[1]School of Information Engineering, Guangdong University of Technology, Guangzhou 510006, China
[2]School of Information Science and Engineering, Southeast University, Nanjing 210096, China
[3]Division of Computer, Electrical, Mathematical Science and Engineering, KAUST, Thuwal 23955-6900, Kingdom of Saudi Arabia

DOI: 10.1109/JPHOT.2014.2311446

Manuscript received February 8, 2014; revised March 2, 2014; accepted March 4, 2014. Date of publication March 12, 2014; date of current version March 26, 2014. This work was supported in part by a grant from King Abdulaziz City of Science and technology (KACST), by the National Natural Science Foundation of China (NSFC) under Grants 61372096 and 61320106003, by the China High-Tech 863 Plan under Grant 2012AA01A506, and by the Program for Jiangsu Innovation Team. Corresponding author: L. Yang (e-mail: liangyang.guangzhou@gmail.com).

Abstract: Free-space optical (FSO) communication has become a cost-effective method to provide high data rates. However, the turbulence-induced fading limits its application to short-range applications. To address this, we propose a multiuser diversity (MD) FSO scheme in which the *N*th best user is selected and the channel fluctuations can be effectively exploited to produce a selection diversity gain. More specifically, we first present the statistics analysis for the considered system over both weak and strong atmospheric turbulence channels. Based on these statistics, the outage probability, bit-error rate performance, average capacity, diversity order, and coverage are analyzed. Results show that the diversity order for the gamma–gamma fading is $N \min\{\alpha, \beta\}/2$, where N is the number of users, and α and β are the channel fading parameters related to the effective atmospheric conditions of the link.

Index Terms: Atmospheric turbulence, free-space optical communications, gamma-gamma distribution, log-normal channels.

1. Introduction

Recently free-space optical (FSO) communication systems have received considerable attention due to the high capacity ability it offers for the last-mile applications. Operating over unlicensed optical spectrum, FSO techniques can provide the line-of-sight optical transmission with low cost and good security [1]–[3]. However, the distance-dependent atmospheric turbulence and path-loss affect widespread use of FSO systems and limit their application to short-range links.

Until now, to overcome the limitations, several techniques have been proposed in the literature, including error control coding [4], maximum-likelihood sequence estimation [5], and spatial diversity [6]–[10]. Among these techniques, multiple-input multiple-output (MIMO) FSO systems which are equipped with multiple apertures can effectively combat the fading by creating additional spatial

degrees of freedom. For instance, the authors in [6] investigated the outage probability performance of FSO systems with spatial diversity at both sides. Later, bit-error rate (BER) performance expressions for MIMO FSO links for weak or strong atmospheric turbulence channels were derived in [7], [8]. Recently, circular MIMO FSO nodes with transmit selection and receive generalized selection diversity was investigated in [9]. More recently, the error rate performance comparison of the coherent and subcarrier intensity modulated optical wireless communications was analyzed in [10]. However, the deployment of multiple apertures may increase the system complexity and cost. Furthermore, the distance between the apertures should be separated sufficiently to obtain the uncorrelated channels. Therefore, the concept of cooperative diversity which has been extensively studied in the conventional radio frequency (RF) communications was applied to the FSO systems. Such a relay-assisted transmission can create a virtual multiple-aperture system and realize the advantages of MIMO technique. As a result, the performance analysis of relay-assisted FSO transmission has been extensively studied for both amplify-and-forward (AF) and decode-and-forward (DF) modes over different channel models (serial or parallel) [11]–[16].

Except the above mentioned techniques, in a point-to-multipoint wireless system, multiuser diversity (MD) can also be exploited to provide multiuser diversity gain which can improve the system throughput and hence the link reliability significantly [17]. The basic idea of MD is to take advantage of the channel fluctuations to obtain a certain performance gain. Such a technique has been extensively considered for RF systems subject to multipath fading and shadowing. Similarly, since the performance of FSO systems depends strongly on the atmospheric conditions and the rapid channel fluctuations between the transmitter and the receiver, MD can also be used to offer a selection diversity gain.

In this paper, a novel FSO communication system is developed where the transmitter communicates with multi-receivers and the Nth best user is selected as the target user. To the best of the authors' knowledge, multiuser diversity scheduling in FSO communications has been recently considered only in [18]. In this work, the authors focused on the scheduling policies and only the user with the best channel quality is selected. In this paper, we consider a more general selection scheme where the Nth best user is selected. The reason is that sometimes the user with best channel conditions does not have data to transmit under given traffic conditions. Therefore, the scheduler can select the second best or generally the Nth best user. It should be noted that such a selection scheme includes the best user selection scheme, as a special case. Our performance metrics are the average capacity, outage probability, and the BER. More specifically, we first derive some statistical characteristics for two turbulence conditions: weak (log-normal distribution) and strong (gamma-gamma distribution). Then, with this in hand, the analysis for average capacity, outage probability, and BER are presented. Finally, some numerical results are provided to verify our analysis.

2. System and Channel Models

We consider a FSO communication system with K users as depicted in Fig. 1 and in which the central node is equipped with K apertures and the users are only equipped with single apertures. Each aperture k at the central node is directed to the optical receiver k. Signals are transmitted from the aperture k to the target user k through the turbulence-induced fading channels and are corrupted at the receiver by the additive noise. In this work, we restrict our analysis to be background noise limited and the noise is modeled as additive white Gaussian noise with zero mean and power spectral density N_0. We also assume that the system uses intensity modulation direct-detection (IM/DD) with on-off keying (OOK) modulation.

2.1. Channel Model

In this work, we consider an aggregated channel model where both the turbulence-induced fading and the path-loss are included. For the kth link between the kth aperture at the transmitter and the kth user, the channel with distance d_k can be modeled as [11], [13], [16]

$$h_k = L(d_k)\tilde{h}_k, \tag{1}$$

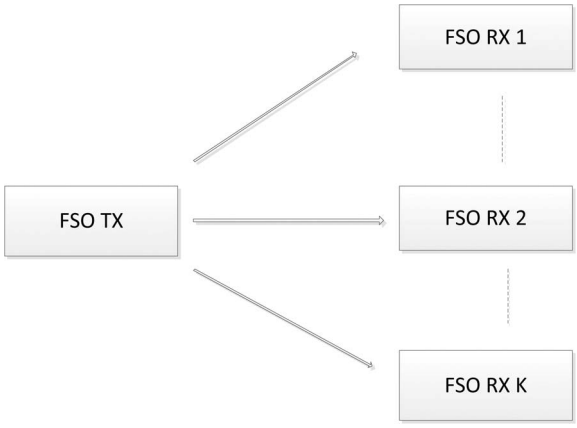

Fig. 1. Diagram of a multiuser FSO communication system.

where $\tilde{h}_k$ represents the atmospheric fading term and $L(d_k)$ denotes the path-loss and can be written as [13]

$$L(d_k) = \frac{D_R^2}{(D_T + \theta_T d_k)^2} e^{-v d_k}, \tag{2}$$

where D_R and D_T are the receiver and transmitter aperture diameters, v is the weather-dependent attenuation coefficient, and θ_T is the optical beam's divergence angle, respectively. With (1), the instantaneous electrical signal-to-noise (SNR) can be defined as [11], [13]

$$\gamma_k = \bar{\gamma}_k |\tilde{h}_k|^2, \tag{3}$$

where $\bar{\gamma}_k$ is the average SNR of link k. In the FSO communication context, such a fading can be modeled by two different distributions, i.e., log-normal distribution for weak atmospheric turbulence and gamma-gamma distribution for strong atmospheric turbulence. In what follows, and for notation simplicity, we use LN and GG to denote the log-normal distribution and gamma-gamma distribution, respectively.

2.1.1. Log-Normal Distribution

As mentioned above, for weak turbulence conditions, the fading is commonly modeled by a log-normal distribution [11], [12], [14]–[16]. Namely, $|\tilde{h}_k| = e^{X_k}$ and $|\tilde{h}_k|^2 = e^{2X_k}$, where X_k is normally distributed with mean μ_{X_k} and variance $\sigma^2_{X_k}$. To guarantee that the fading coefficients conserve the power, we have $E[|\tilde{h}_k|^2] = 1$, which implies $\mu_{X_k} = -\sigma^2_{X_k}$ [11]. Therefore, the probability density function (PDF) of γ_k is given by

$$f^{LN}_{\gamma_k}(\gamma) = \frac{1}{2\gamma\sqrt{2\pi\sigma^2_{X_k}}} \exp\left(-\frac{\left(\ln\left(\frac{\gamma}{\bar{\gamma}_k}\right) + 2\sigma^2_{X_k}\right)^2}{8\sigma^2_{X_k}}\right), \tag{4}$$

and its corresponding cumulative density function (CDF) can be written as

$$F^{LN}_{\gamma_k}(\gamma) = 1 - Q\left(\frac{\ln\left(\frac{\gamma}{\bar{\gamma}_k}\right) + 2\sigma^2_{X_k}}{2\sigma_{X_k}}\right), \tag{5}$$

where $Q(\cdot)$ is the Gaussian-Q function defined as $Q(y) = 1/\sqrt{2\pi}\int_y^\infty \exp(-t^2/2)dt$. The log-normal variance is given by [20]

$$\sigma_{X_k}^2 = \exp\left[\frac{0.49\delta^2}{(1+0.18L^2+0.56\delta^{12/5})^{7/6}} + \frac{0.51\delta^2}{(1+0.9L^2+0.62L^2\delta^{12/5})^{5/6}}\right] - 1, \tag{6}$$

where the Rytov variance $\delta^2 = 1.23C_n^2(2\pi/\lambda)^{7/6}d_k^{11/6}$, C_n^2 is the refractive index structure constant given by [19], λ is the wavelength, and $L = \sqrt{2\pi D_R^2/(4d_k\lambda)}$. Note that the value of C_n^2 depends on the atmospheric turbulence strength.

2.1.2. Gamma-Gamma Distribution

For strong atmospheric condition, the channel fading can be modeled using the well-known gamma-gamma distribution [8], [13], [20]. Thus, the PDF of $|\tilde{h}_k|$ is readily given by [13], [20]

$$f_{|\tilde{h}_k|}^{GG}(x) = \frac{2(\alpha\beta)^{\frac{\alpha+\beta}{2}}}{\Gamma(\alpha)\Gamma(\beta)} x^{\frac{\alpha+\beta}{2}-1} K_{\alpha-\beta}(2\sqrt{\alpha\beta x}), \tag{7}$$

where $\Gamma(\cdot)$ is the gamma function, and α and β are the fading parameters related to the effective atmospheric conditions of the link and depend on the Rytov variance, and $K_v(x)$ is the modified Bessel function of the second kind of order v. More specifically, from [20], the values of α and β can be expressed as $\alpha = \exp[(0.49\delta^2/(1+0.18L^2+0.56\delta^{12/5})^{7/6})-1]^{-1}$ and $\beta = \exp[(0.51\delta^2/(1+0.9L^2+0.62L^2\delta^{12/5})^{5/6})-1]^{-1}$. By applying a simple variable transformation, the PDF of γ_k can be obtained as [20]

$$f_{\gamma_k}^{GG}(\gamma) = \frac{(\alpha\beta)^{\frac{\alpha+\beta}{2}}\bar{\gamma}_k^{-\frac{\alpha+\beta}{4}}}{\Gamma(\alpha)\Gamma(\beta)} \gamma^{\frac{\alpha+\beta}{4}-1} K_{\alpha-\beta}\left(2\sqrt{\alpha\beta\sqrt{\frac{\gamma}{\bar{\gamma}_k}}}\right), \tag{8}$$

and its corresponding CDF is given by

$$F_{\gamma_k}^{GG}(\gamma) = \frac{1}{\Gamma(\alpha)\Gamma(\beta)} G_{1,3}^{2,1}\left[\alpha\beta\sqrt{\frac{\gamma}{\bar{\gamma}_k}}\Big|_{\alpha,\beta,0}^{1}\right], \tag{9}$$

where $G_{p,q}^{m,n}(x|_{b_1,\ldots,b_q}^{a_1,\ldots,a_p})$ is the Meijer's G-function [21].

If the transmitter can collect all of the information γ_k, we assume that the Nth best user is selected. Such a selection scheme has been discussed for RF systems [22], [23]. The reason of using such a selection scheme is that sometimes the conventional best user selection is not available for transmission. Let $\gamma_{1,K} \le \gamma_{2,K} \le \cdots \le \gamma_{K,K}$ denote the order statistics obtained by arranging the random variables γ_k in an increasing order of magnitude. For tractable analysis, we assume that γ_k are independent and identically distributed, i.e., $\bar{\gamma}_k = \bar{\gamma}$ for all users. Then, the CDF and PDF of the Nth order statistic $\gamma_{N,K}$ are given by [24]

$$F_{\gamma_{N,K}}(\gamma) = \sum_{i=N}^{K}\binom{K}{i}\left[F_{\gamma_k}(\gamma)\right]^i\left[1-F_{\gamma_k}(\gamma)\right]^{K-i} \tag{10}$$

$$f_{\gamma_{N,K}}(\gamma) = \frac{K!\left[F_{\gamma_k}(\gamma)\right]^{N-1}\left[1-F_{\gamma_k}(\gamma)\right]^{K-N}f_{\gamma_k}(\gamma)}{(N-1)!(K-N)!}, \tag{11}$$

where $f_{\gamma_k}(\gamma)$ and $F_{\gamma_k}(\gamma)$ have been given in (4), (5) and (8), (9), respectively. Note that such a scheme usually needs that all the estimated channel state information (CSI) is sent back to the transmitter via a low-rate error-free feedback link.

2.2. Statistical Characteristics

In this subsection, we will derive the resulting CDF and PDF expressions for both the log-normal and the gamma-gamma distributions.

First note that for $K \geq 2$, using the exact CDF formulas (5) and (9) to evaluate the system performance is very complicated. Therefore, we need to find approximate expressions for both the CDF and PDF in both weak and strong turbulence conditions.

2.2.1. Weak Turbulence Condition

Consider now the log-normal distribution model. From [25], the $Q(\cdot)$ function can be approximated by

$$Q(x) \approx \frac{1}{12}\exp\left(-\frac{x^2}{2}\right) + \frac{1}{4}\exp\left(-\frac{2x^2}{3}\right) \quad x \geq 0. \tag{12}$$

Using this approximation and letting $2\sigma_X^2 - \ln(\bar{\gamma}) = \mu$ for notation simplicity, the CDF of $\gamma_{N,K}$ for the log-normal case can be shown based on (5), (10), and (12) and some manipulation to be given by

$$F_{\gamma_{N,K}}^{LN}(\gamma) \approx \sum_{i=N}^{K}\sum_{j=0}^{i}\sum_{n=0}^{j}\sum_{t=0}^{K-i}\binom{K}{i}\binom{i}{j}\binom{j}{n}\binom{K-i}{t}\cdot\frac{(-1)^j}{12^{j-n+K-i-t}4^{n+t}} \times \exp\left(-\frac{(3(K-i+j)+n+t)(\ln(\gamma)+\mu)^2}{24\sigma_X^2}\right), \quad \gamma > \bar{\gamma}e^{-2\sigma_X^2}. \tag{13}$$

Similarly, combining (4), (11) and (12), we obtain the PDF of $\gamma_{N,K}$ as

$$f_{\gamma_{N,K}}^{LN}(\gamma) \approx \frac{K!}{(N-1)!(K-N)!}\sum_{j=0}^{N-1}\sum_{n=0}^{j}\sum_{t=0}^{K-N}\binom{N-1}{j}\binom{j}{n}\cdot\binom{K-N}{t}\frac{(-1)^j}{12^{j-n+K-N-t}4^{n+t}}\frac{1}{2\sigma_X\sqrt{2\pi}\gamma} \cdot \exp\left(-\frac{(3(K-N+j+1)+n+t)(\ln(\gamma)+\mu)^2}{24\sigma_X^2}\right), \quad \gamma > \bar{\gamma}e^{-2\sigma_X^2}. \tag{14}$$

Since the approximate expression (12) is only applicable for $x \geq 0$, it requires that $\ln(\gamma/\bar{\gamma}) + 2\sigma_X^2 > 0$ in (5). This means that (13) and (14) are applicable only to the low SNR regime. To make our results applicable for the whole SNR range, we should derive the result for $\ln(\gamma/\bar{\gamma}) + 2\sigma_X^2 < 0$ case. From (5), we can easily see that for this case

$$F_{\gamma_k}^{LN}(\gamma) = Q\left(-\frac{\ln(\gamma)+\mu}{2\sigma_X}\right), \qquad 0 < \gamma < \bar{\gamma}e^{-2\sigma_X^2}. \tag{15}$$

Then, using (12) again, we obtain the CDF and PDF of $\gamma_{N,K}$ as

$$F_{\gamma_{N,K}}^{LN}(\gamma) \approx \sum_{i=N}^{K}\sum_{j=0}^{K-i}\sum_{n=0}^{j}\sum_{t=0}^{i}\binom{K}{i}\binom{K-i}{j}\binom{j}{n}\binom{i}{t}\frac{(-1)^j}{12^{j-n+i-t}4^{n+t}} \times \exp\left(-\frac{(3(i+j)+n+t)(\ln(\gamma)+\mu)^2}{24\sigma_X^2}\right), \qquad 0 < \gamma < \bar{\gamma}e^{-2\sigma_X^2} \tag{16}$$

$$f_{\gamma_{N,K}}^{LN}(\gamma) \approx \frac{K!}{(N-1)!(K-N)!}\sum_{j=0}^{K-N}\sum_{n=0}^{j}\sum_{t=0}^{N-1}\binom{K-N}{j}\cdot\binom{j}{n}\binom{N-1}{t}\frac{(-1)^j}{12^{j-n+N-1-t}4^{n+t}}\frac{1}{2\sigma_X\sqrt{2\pi}\gamma} \cdot \exp\left(-\frac{(3(N+j)+n+t)(\ln(\gamma)+\mu)^2}{24\sigma_X^2}\right), \qquad 0 < \gamma < \bar{\gamma}e^{-2\sigma_X^2} \tag{17}$$

respectively.

2.2.2. Strong Turbulence Condition

We now focus on the gamma-gamma distribution model and develop an approximate CDF expression. By using [10, Eq. (19)], the CDF in (9) can be rewritten as

$$F_{\gamma_k}^{GG}(\gamma) = \frac{1}{\Gamma(\alpha)\Gamma(\beta)} \frac{\pi}{2\sin((\alpha-\beta)\pi)} \sum_{s=0}^{\infty} \left[\frac{2}{(s+\beta)\Gamma(\beta-\alpha+1+s)s!} \left(\frac{\alpha\beta}{\sqrt{\bar{\gamma}}}\right)^{s+\beta} \gamma^{\frac{s+\beta}{2}} - \frac{2}{(s+\alpha)\Gamma(\alpha-\beta+1+s)s!} \left(\frac{\alpha\beta}{\sqrt{\bar{\gamma}}}\right)^{s+\alpha} \gamma^{\frac{s+\alpha}{2}} \right]. \quad (18)$$

It should be noted that $\beta - \alpha$ is not an integer in (18). In practice, it is sufficient to use a high enough number M of items to compute the CDF in (18). Substituting (18) into (10), we get the CDF of the SNR of a gamma-gamma modeled FSO system with the Nth best user selection as

$$F_{\gamma_{N,K}}^{GG}(\gamma) \approx \sum_{i=N}^{K} \sum_{j=0}^{i} \sum_{p=0}^{M(i-j)} \sum_{q=0}^{Mj} \sum_{t=0}^{K-i} \sum_{r=0}^{t} \sum_{a=0}^{M(t-r)} \sum_{b=0}^{Mr} \binom{K}{i} \binom{i}{j} \binom{K-i}{t} \binom{t}{r} (-1)^{j+t+r} \eta_p \eta_q \lambda_a \lambda_b \times \left(\frac{1}{\Gamma(\alpha)\Gamma(\beta)} \frac{\pi}{2\sin((\alpha-\beta)\pi)} \right)^{i+t} \left(\alpha\beta \sqrt{\frac{\gamma}{\bar{\gamma}}} \right)^{\beta(i-j+t-r)+\alpha(j+r)+p+q+a+b}, \quad (19)$$

where η_p, η_q, λ_a, and λ_b are the coefficients of $(\alpha\beta\sqrt{(\gamma/\bar{\gamma})})^p$, $(\alpha\beta\sqrt{(\gamma/\bar{\gamma})})^q$, $(\alpha\beta\sqrt{(\gamma/\bar{\gamma})})^a$, and $(\alpha\beta\sqrt{(\gamma/\bar{\gamma})})^b$ in the expansions of

$$\left[\sum_{s=0}^{M} \frac{2}{(s+\beta)\Gamma(\beta-\alpha+1+s)s!} \left(\alpha\beta \sqrt{\frac{\gamma}{\bar{\gamma}}} \right)^s \right]^{i-j}$$

$$\left[\sum_{s=0}^{M} \frac{2}{(s+\alpha)\Gamma(\alpha-\beta+1+s)s!} \left(\alpha\beta \sqrt{\frac{\gamma}{\bar{\gamma}}} \right)^s \right]^{j}$$

$$\left[\sum_{s=0}^{M} \frac{2}{(s+\beta)\Gamma(\beta-\alpha+1+s)s!} \left(\alpha\beta \sqrt{\frac{\gamma}{\bar{\gamma}}} \right)^s \right]^{t-r}$$

$$\left[\sum_{s=0}^{M} \frac{2}{(s+\alpha)\Gamma(\alpha-\beta+1+s)s!} \left(\alpha\beta \sqrt{\frac{\gamma}{\bar{\gamma}}} \right)^s \right]^{r}$$

respectively. Next we will use the derived PDF and CDF expressions to analyze the performance of the system under consideration.

3. Performance Analysis

In this section, we present performance analysis for FSO communication systems with MD. More specifically, the outage probability, BER, average capacity, diversity order, and coverage are derived.

3.1. Outage Probability Analysis

In wireless communication, outage probability is an important performance metric and is defined as the probability that the instantaneous SNR γ_{k^*} falls below a given threshold SNR γ_{th}. Recall that the outage probability is related to the derived CDF expressions. Therefore, the exact outage probability can be simply obtained by replacing γ with γ_{th} in (10) as

$$P_{out} = \sum_{i=N}^{K} \binom{K}{i} \left[F_{\gamma_k}(\gamma_{th}) \right]^i \left[1 - F_{\gamma_k}(\gamma_{th}) \right]^{K-i} \quad (20)$$

where the exact expressions $F_{\gamma_k}(\gamma_{th})$ can be readily obtained from (5) and (9). We also can use the approximate formulas (13), (16), and (19) to evaluate the outage probability performance.

3.2. BER Analysis

From [26], the average BER can be evaluated by using the CDF-based method as

$$P_e = E_X\left\{F_{\gamma_{k^*}}\left(\frac{X^2}{2}\right)\right\} \tag{21}$$

where X is a random variable with standard Normal distribution.

Substituting (13) and (16) into (21), we obtain the approximate BER expressions for the log-normal modeled FSO system with the Nth best user selection at low SNR and high SNR as

$$P_e^{LN-LS} \approx \frac{1}{2}\sum_{i=N}^{K}\sum_{j=0}^{i}\sum_{n=0}^{j}\sum_{t=0}^{K-i}\binom{K}{i}\binom{i}{j}\binom{j}{n}\binom{K-i}{t}\frac{(-1)^j}{12^{j-n+K-i-t}4^{n+t}}\frac{2}{\sqrt{\pi}} \times \int_{e^{-\mu}}^{\infty}\exp\left(-\frac{(3(K-i+j)+n+t)(\ln(y)+0.5\mu)^2}{6\sigma_{X_k}^2}\right)e^{-y^2}dy \tag{22}$$

$$P_e^{LN-HS} \approx \frac{1}{2}\sum_{i=N}^{K}\sum_{j=0}^{K-i}\sum_{n=0}^{j}\sum_{t=0}^{i}\binom{K}{i}\binom{K-i}{j}\binom{j}{n}\binom{i}{t}\frac{(-1)^j}{12^{j-n+i-t}4^{n+t}}\frac{2}{\sqrt{\pi}} \times \int_{0}^{e^{-\mu}}\exp\left(-\frac{(3(i+j)+n+t)(\ln(y)+0.5\mu)^2}{6\sigma_X^2}\right)e^{-y^2}dy. \tag{23}$$

To evaluate the above integrals, we define two integrals as

$$I_1(A,B) = \frac{2}{\sqrt{\pi}}\int_0^{\infty}\exp\left(-A(\ln(x)+B)^2\right)\exp(-x^2)\,dx, \qquad A>0 \tag{24}$$

$$I_2(A,B,\lambda) = \frac{2}{\sqrt{\pi}}\int_{\lambda}^{\infty}\exp\left(-A(\ln(x)+B)^2\right)e^{-x^2}dx, \qquad A>0. \tag{25}$$

Two infinite series representations for I_1 and I_2 are given in Appendices A and B. Using these results, we obtain closed-form expressions for (22) and (23) as

$$P_e^{LN-LS} \approx \frac{1}{2}\sum_{i=N}^{K}\sum_{j=0}^{i}\sum_{n=0}^{j}\sum_{t=0}^{K-i}\binom{K}{i}\binom{i}{j}\binom{j}{n}\binom{K-i}{t} \cdot\frac{(-1)^j}{12^{j-n+K-i-t}4^{n+t}}I_2\left(\frac{3(K-i+j)+n+t}{6\sigma_{X_k}^2}, 0.5\mu, e^{-\mu}\right) \tag{26}$$

$$P_e^{LN-HS} \approx \frac{1}{2}\sum_{i=N}^{K}\sum_{j=0}^{K-i}\sum_{n=0}^{j}\sum_{t=0}^{i}\binom{K}{i}\binom{K-i}{j}\binom{j}{n}\binom{i}{t}\frac{(-1)^j}{12^{j-n+i-t}4^{n+t}} \times\left[I_1\left(\frac{3(i+j)+n+t}{6\sigma_X^2}, 0.5\mu\right) - I_2\left(\frac{3(i+j)+n+t}{6\sigma_X^2}, 0.5\mu, e^{-\mu}\right)\right]. \tag{27}$$

Therefore, the total average BER is $P_e^{LN-LS} + P_e^{LN-HS}$.

Similarly, by substituting (19) into (21) and using [21, Eq. (3.326.2)], the average BER over the gamma-gamma modeled optical channel with the Nth best user selection can be obtained as

$$P_e^{GG} \approx \sum_{i=N}^{K}\sum_{j=0}^{i}\sum_{p=0}^{M(i-j)}\sum_{q=0}^{Mj}\sum_{t=0}^{K-i}\sum_{r=0}^{t}\sum_{a=0}^{M(t-r)}\sum_{b=0}^{Mr}\binom{K}{i}\binom{i}{j} \times \binom{K-i}{t}\binom{t}{r}(-1)^{j+t+r}\left(\frac{1}{\Gamma(\alpha)\Gamma(\beta)}\frac{\pi}{2\sin((\alpha-\beta)\pi)}\right)^{i+t} \times \eta_p\eta_q\lambda_a\lambda_b\left(\frac{\alpha\beta}{\sqrt{\bar{\gamma}}}\right)^{\beta(i-j+t-r)+\alpha(j+r)+p+q+a+b} \times \frac{1}{2\sqrt{\pi}}\Gamma\left(\frac{\beta(i-j+t-r)+\alpha(j+r)+p+q+a+b+1}{2}\right). \quad (28)$$

3.3. Average Capacity Analysis

For a wireless fading channel, the average capacity can be evaluated as

$$\langle C\rangle = \frac{1}{\ln(2)}\int_0^\infty \ln(1+\gamma) f_{\gamma_{N,K}}(\gamma)\, d\gamma. \quad (29)$$

Exact closed-form expressions for the above integrals are not available and as such numerical integration should be used. In the following, we derive tight approximate capacity expressions.

Let us first consider the log-normal case. Combining (4), (5), (11) and (29), we obtain

$$C^{LN} = \frac{1}{2\sigma_X\sqrt{2\pi}\ln(2)}\frac{K!}{(N-1)!(K-N)!}\int_0^\infty \left[1-Q\left(\frac{\ln(\gamma)+\mu}{2\sigma_X}\right)\right]^{N-1} \times \left[Q\left(\frac{\ln(\gamma)+\mu}{2\sigma_X}\right)\right]^{K-N}\frac{1}{\gamma}\exp\left(-\frac{(\ln(\gamma)+\mu)^2}{8\sigma_X^2}\right)\ln(1+\gamma)\, d\gamma. \quad (30)$$

By using the change of variable $y = \ln(\gamma)+\mu$, (30) can be rewritten as

$$C^{LN} = \frac{1}{2\sigma_X\sqrt{2\pi}\ln(2)}\frac{K!}{(N-1)!(K-N)!}\int_{-\infty}^\infty \left[1-Q(\sqrt{2}x)\right]^{N-1} \times \left[Q(\sqrt{2}x)\right]^{K-N}2\sqrt{2}\sigma_X\exp(-x^2)\ln(1+e^{-\mu}e^{2\sqrt{2}\sigma_X x})\, dx. \quad (31)$$

Applying the Gauss-Hermite integration, the average capacity can be approximated as

$$C^{LN} \approx \frac{1}{\sqrt{\pi}\ln(2)}\frac{K!}{(N-1)!(K-N)!}\sum_{i=1}^{W} w(x_i)\left[1-Q(\sqrt{2}x_i)\right]^{N-1}\left[Q(\sqrt{2}x_i)\right]^{K-N}\ln(1+e^{-\mu}e^{2\sqrt{2}\sigma_X x_i}) \quad (32)$$

where x_i, $w(x_i)$, and W are the abscissas, weights, and the number of Gauss-Hermite integration.

To obtain the capacity for the gamma-gamma fading case, we use the asymptotic formula for the Bessel K-function $K_v(x) \approx (\sqrt{\pi}e^{-x}/\sqrt{2x})$. Then, the PDF (8) can be approximated by

$$f_{\gamma_k}^{GG}(\gamma) \approx \frac{\sqrt{\pi}}{2\Gamma(\alpha)\Gamma(\beta)}\left(\frac{\alpha\beta}{\sqrt{\bar{\gamma}}}\right)^{\frac{\alpha+\beta}{2}-\frac{1}{4}}\gamma^{\frac{\alpha+\beta}{4}-\frac{9}{8}}\exp\left(-2\sqrt{\frac{\alpha\beta}{\sqrt{\bar{\gamma}}}}\gamma^{1/4}\right). \quad (33)$$

After some mathematical manipulation, the CDF can be written as

$$F_{\gamma_k}^{GG}(\gamma) \approx \frac{2\sqrt{\pi}}{\Gamma(\alpha)\Gamma(\beta)} 2^{-\varepsilon} \exp\left(-2\sqrt{\frac{\alpha\beta}{\sqrt{\bar{\gamma}}}\gamma^{1/4}}\right) \cdot \sum_{w=0}^{\infty} \frac{\left(2\sqrt{\frac{\alpha\beta}{\sqrt{\bar{\gamma}}}\gamma^{1/4}}\right)^{\varepsilon+w}}{\varepsilon(\varepsilon+1)\cdots(\varepsilon+w)} \tag{34}$$

where $\varepsilon = \alpha + \beta - 0.5$. Combining (11), (33) and (34), the PDF of FSO communication systems with the Nth best user selection over gamma-gamma fading channels can be obtained as

$$f_{\gamma_{N,K}}^{GG}(\gamma) \approx \frac{K!\sqrt{\pi}}{(N-1)!(K-N)!2\Gamma(\alpha)\Gamma(\beta)} \left(\frac{\alpha\beta}{\sqrt{\bar{\gamma}}}\right)^{\frac{\alpha+\beta}{2}-\frac{1}{4}} \sum_{i=0}^{K-N} \binom{K-N}{i} (-1)^i \left(\frac{2\sqrt{\pi}2^{-\varepsilon}}{\Gamma(\alpha)\Gamma(\beta)}\right)^{N-1+i}$$
$$\cdot \sum_{s=0}^{M(N-1+i)} \lambda_s \left(2\sqrt{\frac{\alpha\beta}{\sqrt{\bar{\gamma}}}}\right)^{\varepsilon(N-1+i)+s} \exp\left(-(N+i)2\sqrt{\frac{\alpha\beta}{\sqrt{\bar{\gamma}}}\gamma^{1/4}}\right) \cdot \gamma^{\frac{\alpha+\beta+\varepsilon(N-1+i)+s}{4}-\frac{9}{8}} \tag{35}$$

where λ_s is the coefficient of $(2\sqrt{(\alpha\beta/\sqrt{\bar{\gamma}})}\gamma^{1/4})^s$ in the expansion of

$$\left(\sum_{w=0}^{M} \frac{\left(2\sqrt{\frac{\alpha\beta}{\sqrt{\bar{\gamma}}}\gamma^{1/4}}\right)^{w}}{\varepsilon(\varepsilon+1)\cdots(\varepsilon+w)}\right)^{N-1+i}.$$

Since $((\alpha+\beta+\varepsilon(N-1+i)+s)/4) - (9/8)$ is not necessary an integer, we can not use the result [27, Eq. (78)] to compute the capacity directly. However, the capacity can be easily computed by using the Gauss-Laguerre integration.

3.4. Diversity Order Analysis

In wireless communication system, the diversity order d is an important parameter to indicate the ability of combating the fading for a given technique. Commonly, this performance is defined as the negative ratio between the BER or outage probability versus the SNR on a log-log scale as $\bar{\gamma} \to \infty$, namely, [28],

$$d = -\lim_{\bar{\gamma}\to\infty} \frac{\log P_{out}(r\log\bar{\gamma})}{\log\bar{\gamma}} \tag{36}$$

where $0 \le r \le 1$ is the multiplexing gain. So, for the log-normal distribution case, since the limitation $\lim_{\bar{\gamma}\to\infty}(\log(1 - Q((r-1)\ln(\bar{\gamma}) + 2\sigma_X^2/2\sigma_X)))/\log\bar{\gamma})$ does not exist, the conventional definition of the diversity gain can not be used for the log-normal fading. We note that such a result has been observed in [16] and the concept of the relative diversity order (RDO) was proposed instead. Using the definition of RDO, we can find that the RDO for our considered system is N.

Now we turn our attention to the gamma-gamma case. If we ignore the higher terms in (18), the outage probability can be rewritten as

$$P_{out}^{GG}(\gamma) \approx \sum_{i=N}^{K} \sum_{j=0}^{i} \sum_{t=0}^{K-i} \sum_{r=0}^{t} \binom{K}{i}\binom{i}{j}\binom{K-i}{t}\binom{t}{r} (-1)^{j+t+r}$$
$$\times \left(\frac{\pi(\Gamma(\alpha)\Gamma(\beta))^{-1}}{2\sin((\alpha-\beta)\pi)}\right)^{i+t} \left(\alpha\beta\sqrt{\frac{\gamma_{th}}{\bar{\gamma}}}\right)^{\beta(i-j+t-r)+\alpha(j+r)}. \tag{37}$$

Since the superscript n of $\bar{\gamma}^{-n}$ reflects the value of the diversity order and the term with the smallest n in the sum expression Eq. (37) dominates the BER, we can conclude that the achievable diversity

order of FSO communication systems over gamma-gamma fading channels with the Nth best user selection is $N \min\{\alpha, \beta\}/2$. If $N = K$, the diversity order will be $K \min\{\alpha, \beta\}/2$. We note that the authors in [10] have presented a diversity order analysis for the MIMO FSO communication systems and they show the diversity order for selective combining (SC) over gamma-gamma fading is $L \min\{\alpha, \beta\}$ where L is the number of branches at the receiver. Notice that the difference of the factor 1/2 is that the authors in [10] use the PDF (7) of this paper to compute the performance, which can be observed from the PDF expressions (7) and (8).

3.5. Coverage Analysis

In this subsection, we investigate the effect of the multiuser scheduling on the coverage. Like [29], we can use the outage probability to analyze the maximum distance under a given SNR threshold γ_{th}. More specifically, the coverage improvement for a FSO communication system due to use of the multiuser diversity over Log-normal fading channels is presented. It should be noted that similar analysis can be done for the gamma-gamma fading case. Also, without loss of generality, we consider a special case $N = K$, which does not affect our observation.

For the single user case, the outage probability can be readily obtained from (5). Since the log-variance and the average SNR $\bar{\gamma}$ are the functions of the distance, the distance d_1 of the single user FSO communication system satisfies

$$1 - P_{out} = Q\left(\frac{\ln\left(\frac{\gamma_{th}}{\bar{\gamma}(d_1)}\right) + 2\sigma_X^2(d_1)}{2\sigma_X(d_1)}\right). \tag{38}$$

Similarly, we have the following expression for the multiuser diversity case as

$$1 - \sqrt[K]{P_{out}} = Q\left(\frac{\ln\left(\frac{\gamma_{th}}{\bar{\gamma}(d_2)}\right) + 2\sigma_X^2(d_2)}{2\sigma_X(d_2)}\right). \tag{39}$$

Since $Q(x)$ is a monotone decreasing function, we get

$$\ln\left(\frac{\gamma_{th}}{\bar{\gamma}(d_1)}\right)^{\frac{1}{2\sigma_X(d_1)}} + \sigma_X(d_1) < \ln\left(\frac{\gamma_{th}}{\bar{\gamma}(d_2)}\right)^{\frac{1}{2\sigma_X(d_2)}} + \sigma_X(d_2). \tag{40}$$

Recall that $\bar{\gamma}(d) \downarrow$ and $\sigma_X(d) \uparrow$ when $d \uparrow$. Then, if we suppose that $d_1 > d_2$, it requires that $(1/2\sigma_X(d_1))\ln(\gamma_{th}/\bar{\gamma}(d_1)) < (1/2\sigma_X(d_2))\ln(\gamma_{th}/\bar{\gamma}(d_2))$. Since $(\gamma_{th}/\bar{\gamma}(d_1)) > (\gamma_{th}/\bar{\gamma}(d_2))$, $(1/2\sigma_X(d_1)) < (1/2\sigma_X(d_2))$, and the inequality $\gamma_{th} < \bar{\gamma}(d)$ exists for most cases, it results in $(1/2\sigma_X(d1))\ln(\gamma_{th}/\bar{\gamma}(d1)) > (1/2\sigma_X(d2))\ln(\gamma_{th}/\bar{\gamma}(d2))$, which contradicts the above requirement. Therefore, we can conclude that $d_1 < d_2$. We can then conclude that the use of the multiuser scheduling in FSO communication system can improve the coverage.

4. Numerical Results

In this section, we illustrate some numerical results to show our analysis for the two different channel models under consideration: log-normal distribution and gamma-gamma distribution. To make our analytical results more available for any cases of optical wireless communication systems, we describe the detailed parameters in the follow. As mentioned in the channel model section, for the gamma-gamma fading, the fading parameters α and β are related to the Rytov variance $\delta^2 = 1.23C_n^2(2\pi/\lambda)^{7/6}d^{11/6}$. From the analytical results, we can see that the performance depends on the values of σ_X^2, α, and β. Therefore, for a fair comparison, we adopt the definitions of σ_X^2, α, and β given in [30] and used in [20], respectively, which makes these three parameters have a relationship with δ^2, the wavelength λ, the aperture diameter D_R of the receiver, and the distance d. More specifically, we set: the wavelength $\lambda = 1.55$ μm, the distance $d = 5$ Km, the atmospheric attenuation $\sigma = 0.01$ 1/Km, and $D_R = D_T = 0.1$ m. Since the value of C_n^2 reflects the turbulence

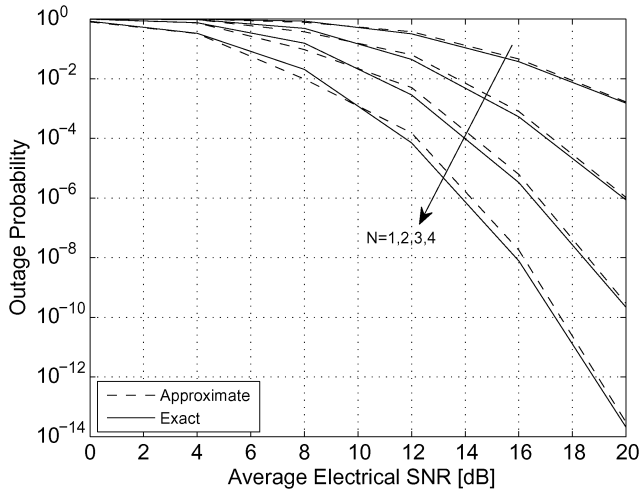

Fig. 2. Outage probability of FSO communication systems with multiuser diversity over weak atmospheric turbulence channels, $C_n^2 = 1 \times 10^{-15}\ m^{-2/3}$.

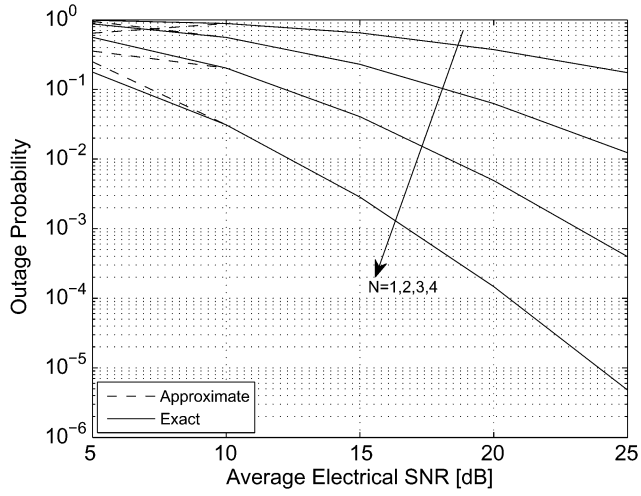

Fig. 3. Outage probability of FSO communication systems with multiuser diversity over strong atmospheric turbulence channels, $C_n^2 = 2 \times 10^{-14}\ m^{-2/3}$.

strength, we present the numerical results for two cases $C_n^2 = 1 \times 10^{-15}\ m^{-2/3}$ and $C_n^2 = 2 \times 10^{-14}\ m^{-2/3}$ which correspond to the weak and strong turbulence conditions, respectively.

In Fig. 2, we plot outage probability curves for the weak turbulence (log-normal fading) by using the exact and approximate formulas when $K = 4$, $N = 1, 2, 3, 4$, and $\gamma_{th} = 5$ dB. The outage probability for the strong turbulence (gamma-gamma fading) is presented in Fig. 3, where we set $K = 4$, $N = 1, 2, 3, 4$, and $\gamma_{th} = 5$ dB. From Figs. 2 and 3, we can see that our proposed approximate analysis is quite accurate. In Fig. 4, we show a comparison between the weak and strong turbulence when $N = K = 6$ and $\gamma_{th} = 3$ dB. It is clearly observed that the strong turbulence has a higher outage performance. In Figs. 5–7, the BER curves are plotted by using the same parameters used in Figs. 2–4. As expected, similar observations can be obtained as those in Figs. 2–4. The average capacity obtained according to the exact and approximate formulas is shown in Fig. 8 where we set $N = K = 4$. We can see that the approximate values are upper bounds. In Fig. 9, we plot the average capacity curves for weak and strong turbulence when $N = K = 1, 4$. For the single user case, we can see that the capacity of the FSO communication systems in weak turbulence is higher than that of the

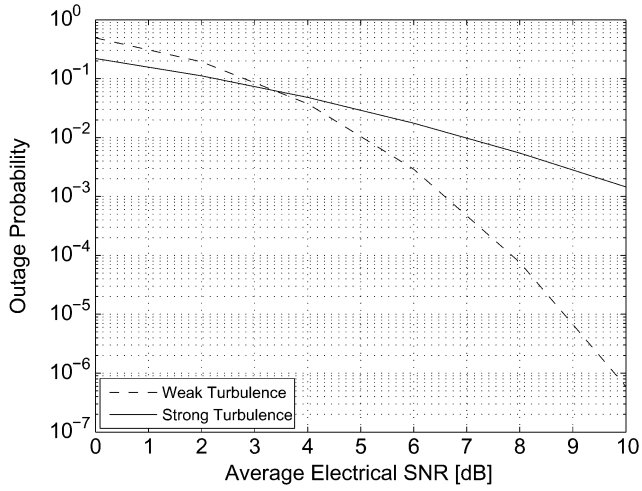

Fig. 4. Outage probability comparison between weak and strong atmospheric turbulence channels when $N = K = 6$.

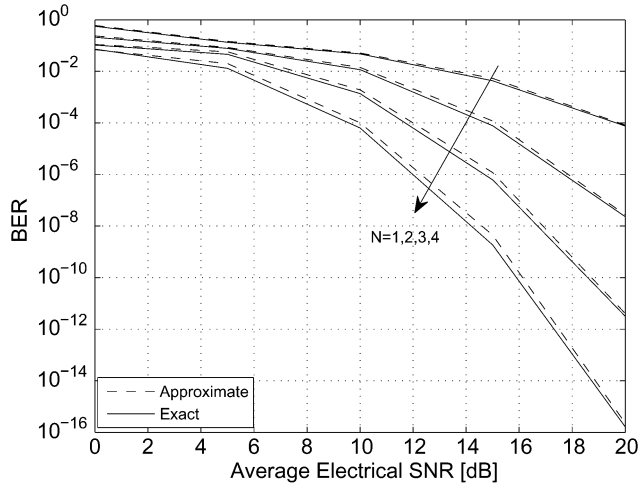

Fig. 5. BER of FSO communication systems with multiuser diversity over weak atmospheric turbulence channels, $C_n^2 = 1 \times 10^{-15}\ m^{-2/3}$.

strong turbulence, which is in agreement with the observation shown in [20]. However, an interesting observation happens for $N = K = 4$ from Figs. 8 and 9. We can find that the strong turbulence has a higher system capacity. The main reason is that the strong turbulence provides more channel fluctuations, which in turn results in a higher multiuser diversity gain and produces a higher throughput. The average capacity versus K is presented in Fig. 10. Again, we can see that the weak turbulence has a higher capacity only at $K = 1$. Also, the capacity increases with the increase of the number of users. Moreover, we can observe that the asymptote is approached and the capacity will become saturated at large K. The reason is that the source of the multiuser diversity gain is the channel fluctuations. Increasing the number of users means increasing the number of channels, which in turn increases the chance of producing larger channel fluctuations. However, the size of cell is limited and more aggregated users may cause small difference between the channels. Therefore, the corresponding multiuser diversity gain will become stable. Finally, from Figs. 4, 7, and 9, we can see that there are some intersections for the comparisons between the strong and weak turbulence. This can be intuitively explained as follows. Recall that the selection metric is $\max_{1 \le k \le K} \bar{\gamma} |h_k|^2$. At low

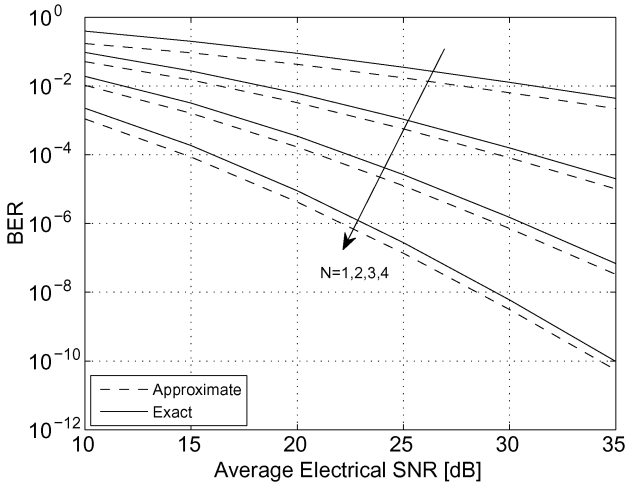

Fig. 6. BER of FSO communication systems with multiuser diversity over strong atmospheric turbulence channels, $C_n^2 = 2 \times 10^{-14}\ m^{-2/3}$.

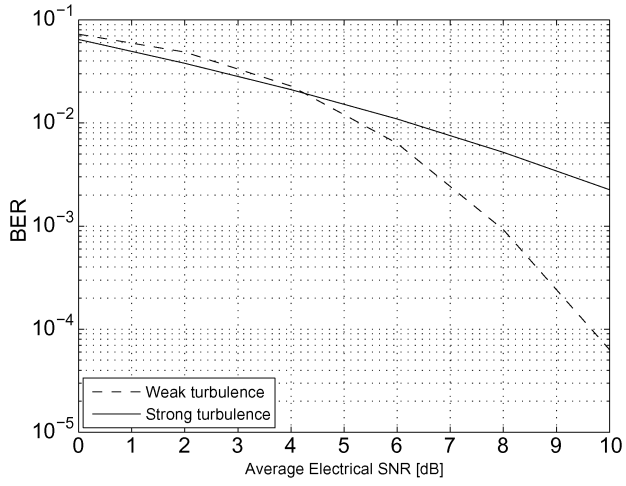

Fig. 7. BER comparison between weak and strong atmospheric turbulence channels when $N = K = 6$.

or mediate SNRs, the MD gain is dominant and can make the strong turbulence case has a better system performance. However, with the increase of the transmit powers, the strength of the channel fluctuations for both strong and weak turbulence cases will be enhanced and the MD gain difference between them will be smaller. Then, the link fading is the main factor affecting the system performance. Therefore, with the increase of the average SNR, the resulting SNR $\bar{\gamma}|h_{k^*}|^2$ for weak turbulence after user selection may be higher than that of the strong turbulence, which makes the weak turbulence has a good system performance.

5. Conclusion

In this paper, we presented a comprehensive performance analysis for the FSO communication systems with MD over both weak and strong atmospheric turbulence. More specifically, we derived some approximate expressions for the outage probability and BER. Results show that the approximate analysis are quite accurate. Furthermore, we observed that with multiuser diversity strong turbulence can yield a higher capacity.

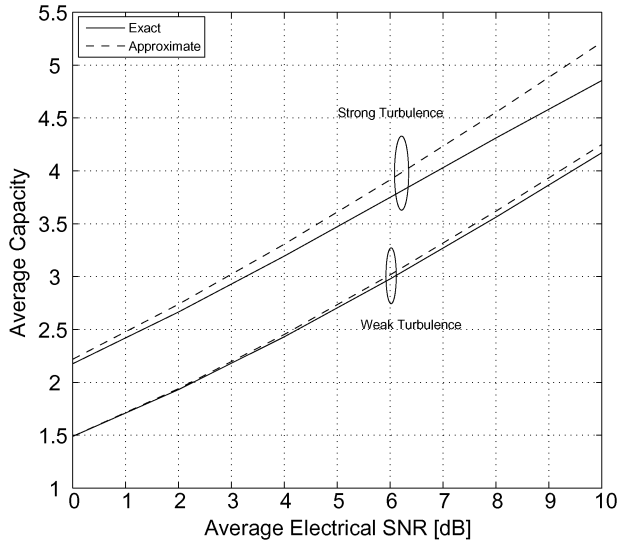

Fig. 8. Average capacity of FSO communication systems with MD when $N = K = 4$.

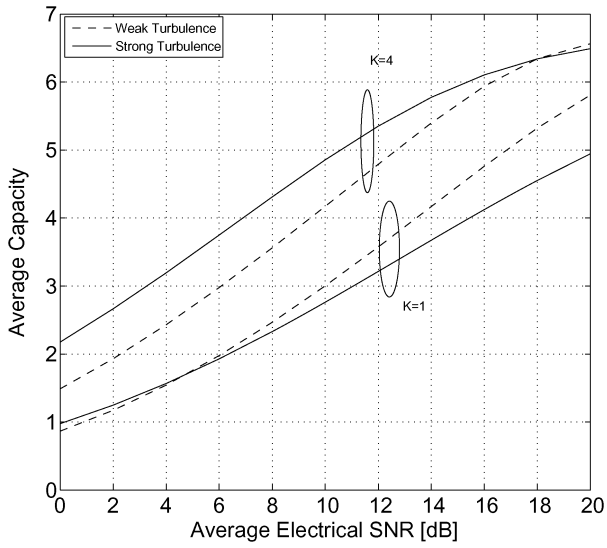

Fig. 9. Average capacity comparison between weak and strong atmospheric turbulence channels when $N = K$.

Appendix I
Evaluation of Integral I_1

Using integration by parts, the integral I_1 can be expressed as

$$I_1 = \lim_{x\to\infty}\mathrm{erf}(x)\exp\left(-A(\ln(x)+B)^2\right) - \lim_{x\to 0}\mathrm{erf}(x)\exp\left(-A(\ln(x)+B)^2\right) + 2A\int_0^{\infty}\mathrm{erf}(x)\exp\left(-A(\ln(x)+B)^2\right)(\ln(x)+B)\frac{1}{x}\,dx. \quad (41)$$

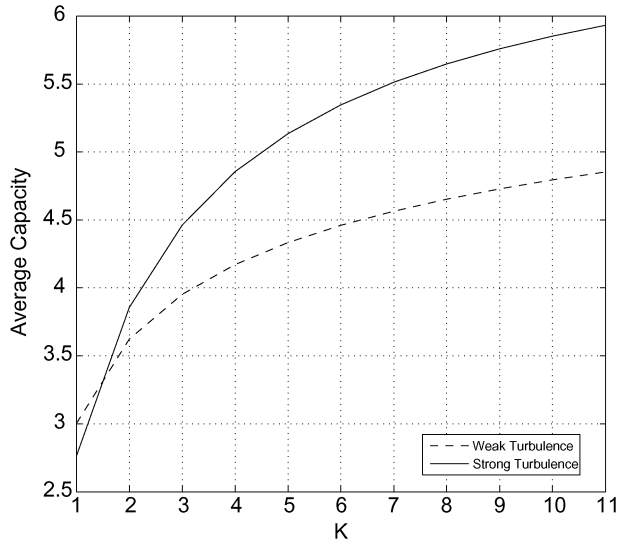

Fig. 10. Average capacity versus K over weak and strong atmospheric turbulence channels when $N = K$.

Since $\text{erf}(0) = 0$ and $\lim_{x\to\infty}\text{erf}(x) = 1$, the first two terms of the right side are zeros. Therefore, the integral I_1 becomes

$$I_1 = 2A\int_0^{\infty} \text{erf}(x)\exp\left(-A(\ln(x)+B)^2\right)(\ln(x)+B)\frac{1}{x}\,dx. \tag{42}$$

By using the fact [21, Eq. (3.321.1)], (42) can be rewritten as

$$I_1 = 2A\frac{2}{\sqrt{\pi}}\sum_{w=0}^{\infty}\frac{(-1)^w}{w!(2w+1)}\int_0^{\infty} x^{2w}\exp\left(-A(\ln(x)+B)^2\right)(\ln(x)+B)dx. \tag{43}$$

Applying the change of the variable $y = \ln(x) + B$, we obtain

$$I_1 = 2A\frac{2}{\sqrt{\pi}}\sum_{w=0}^{\infty}\frac{(-1)^w}{w!(2w+1)}e^{-(2w+1)B}\int_{-\infty}^{\infty} e^{(2w+1)y}\exp(-Ay^2)y\,dy. \tag{44}$$

Using [21, Eq. (3.462.6)], we finally obtain the following expression for I_1

$$I_1 = \frac{2}{\sqrt{A}}\sum_{w=0}^{\infty}\frac{(-1)^w}{w!}e^{-(2w+1)B}\exp\left(\frac{(w+0.5)^2}{A}\right). \tag{45}$$

Appendix II
Evaluation of Integral I_2

Similarly, using integration by parts, the integral I_2 can be expressed as

$$I_2 = \lim_{x\to\infty}\text{erf}(x)\exp\left(-A(\ln(x)+B)^2\right) - \lim_{x\to\lambda}\text{erf}(x)\exp\left(-A(\ln(x)+B)^2\right) + 2A\int_{\lambda}^{\infty}\text{erf}(x)\exp\left(-A(\ln(x)+B)^2\right)(\ln(x)+B)\frac{1}{x}\,dx. \tag{46}$$

Since $\lim_{x\to\infty}\text{erf}(x)=1$, the first term of the right side is zero. Therefore, the integral I_2 becomes

$$I_2 = 2A\int_0^{\infty}\text{erf}(x)\exp\Big(-A(\ln(x)+B)^2\Big)(\ln(x)+B)\frac{1}{x}\,dx - \text{erf}(\lambda)\exp\Big(-A(\ln(\lambda)+B)^2\Big). \quad (47)$$

By using the fact [21, Eq. (3.321.1)], (47) can be rewritten as

$$I_2 = -\text{erf}(\lambda)\exp\Big(-A(\ln(\lambda)+B)^2\Big) + 2A\frac{2}{\sqrt{\pi}}\sum_{w=0}^{\infty}\frac{(-1)^w}{w!(2w+1)} \times \int_{\lambda}^{\infty} x^{2w}\exp\Big(-A(\ln(x)+B)^2\Big)(\ln(x)+B)dx. \quad (48)$$

Applying the change of the variable $y=\ln(x)+B$, we obtain

$$I_2 = -\text{erf}(\lambda)\exp\Big(-A(\ln(\lambda)+B)^2\Big) + 2A\frac{2}{\sqrt{\pi}}\sum_{w=0}^{\infty}\frac{(-1)^w}{w!(2w+1)}e^{-(2w+1)B}\int_{\ln(\lambda)+B}^{\infty} e^{(2w+1)y}\exp(-Ay^2)y\,dy. \quad (49)$$

After some mathematical manipulation, we finally obtain the following expression for I_2

$$I_2 = -\text{erf}(\lambda)\exp\Big(-A(\ln(\lambda)+B)^2\Big) + 2A\frac{2}{\sqrt{\pi}}\sum_{w=0}^{\infty}\frac{(-1)^w}{w!(2w+1)}\cdot e^{-(2w+1)B} \times\left[\frac{e^{-(\ln(\lambda)+B)(A(\ln(\lambda)+B)+2w+1)}}{2A} - \frac{\sqrt{\pi}(2w+1)e^{\frac{(2w+1)^2}{4A}}}{4A^{1.5}}\times\left(1-\text{erf}\left(\sqrt{A}(\ln(\lambda)+B)+\frac{2w+1}{2\sqrt{A}}\right)\right)\right]. \quad (50)$$

References

[1] D. Kedar and S. Arnon, "Urban optical wireless communication networds: The main challengers and possible solutions," *IEEE Commun. Mag.*, vol. 42, no. 5, pp. s2–s7, May 2004.

[2] Advanced Optical Wireless Communication, S. Arnon, J. R. Barry, G. K. Karagiannidis, R. Schober, and M. Uysal, Eds. Cambridge, U.K.: Cambridge Univ. Press, 2012.

[3] L. Andrews and R. L. Philips, *Laser Beam Propagation Through Randowm Media*. Bellingham, WA, USA: SPIE Press, 2005.

[4] X. Zhu and J. M. Kahn, "Performance bounds for coded free-space optical communications through atmospheric turbulence channels," *IEEE Trans. Commun.*, vol. 51, no. 8, pp. 1233–1239, Aug. 2003.

[5] X. Zhu and J. M. Kahn, "Markov chain model in maximum-likelihood sequence detection for free-space optical communication through atmospheric turbulence channels," *IEEE Trans. Commun.*, vol. 51, no. 3, pp. 509–516, Mar. 2003.

[6] E. J. Lee and V. W. S. Chan, "Optical communication over the clear atmospheric channel using diversity," *IEEE J. Sel. Areas Commun.*, vol. 22, no. 9, pp. 1896–1906, Nov. 2004.

[7] S. M. Navidpour, M. Uysal, and M. Kavehrad, "BER performance of free-space optical transmission with spatial diversity," *IEEE Trans. Wireless Commun.*, vol. 6, no. 8, pp. 2813–2819, Aug. 2007.

[8] T. A. Tsiftsis, H. G. Sandalidis, G. K. Karagiannidis, and M. Uysal, "Optical wireless links with spatial diversity over strong atmospheric turbulence channels," *IEEE Trans. Wireless Commun.*, vol. 8, no. 2, pp. 951–957, Feb. 2009.

[9] H. Moradi, H. H. Refai, and P. G. LoPresti, "Circular MIMO FSO nodes with transmit selection and receive generalized selection diversity," *IEEE Trans. Veh. Technol.*, vol. 61, no. 3, pp. 1174–1181, Mar. 2012.

[10] M. Liu, J. Cheng, and J. F. Holzman, "Error rate performance comparison of coherent and subcarrier intensity modulated optical wireless communications," *IEEE/OSA J. Opt. Commun. Netw.*, vol. 5, no. 6, pp. 554–564, Jun. 2013.

[11] M. Safari and M. Uysal, "Relay-assisted free-space optical communication," *IEEE Trans. Wireless Commun.*, vol. 7, no. 12, pp. 5441–5449, Dec. 2008.

[12] M. A. Kashani, M. M. Rad, M. Safari, and M. Uysal, "All-optical amplify-and-forward relaying system for atmospheric channels," *IEEE Commun. Lett.*, vol. 16, no. 10, pp. 1684–1686, Oct. 2012.

[13] N. D. Chatzidiamantis, D. S. Michalopoulos, E. E. Kriezis, G. K. Karagiannidis, and R. Schober, "Relay selection protocols for relay-assisted free-space optical systems," *IEEE/OSA J. Opt. Commun. Netw.*, vol. 5, no. 1, pp. 92–103, Jan. 2013.

[14] M. Karimi and M. Nasiri-kenari, "Free space optical communications via optical amplify-and-forward relaying," *IEEE/OSA J. Lightw. Technol.*, vol. 29, no. 2, pp. 242–248, Jan. 2011.
[15] S. Kazemlou, S. Hranilovic, and S. Kumar, "All-optical multihop free-space optical communication system," *IEEE/OSA J. Lightw. Technol.*, vol. 29, no. 18, pp. 2663–2669, Sep. 2011.
[16] M. A. Kashani, M. Safari, and M. Uysal, "Optimal relay placement and diversity analysis of relay-assisted free-space optical communication systems," *IEEE/OSA J. Opt. Commun. Netw.*, vol. 5, no. 1, pp. 37–47, Jan. 2013.
[17] W. Ajib and D. Haccoun, "An overview of scheduling algorithms in MIMO-based fourth-generation wireless systems," *IEEE Netw.*, vol. 19, no. 5, pp. 43–48, Sep/Oct. 2005.
[18] J. Abouei and K. N. Plataniotis, "Multiuser diversity scheduling in free-space optical communications," *IEEE/OSA J. Lightw. Technol.*, vol. 30, no. 9, pp. 1351–1358, May 2012.
[19] L. Andrews, R. Phillips, and C. Hopen, *Laser Beam Scintillation with Applications*. Bellingham, WA, USA: SPIE Press, 2001.
[20] H. E. Nistazakis, E. A. karagianni, A. D. Tsigopoulos, M. E. Fafalios, and G. S. Tombras, "Average capacity of optical wireless communication systems over atmospheric turbulence channels," *IEEE/OSA J. Lightw. Technol.*, vol. 27, no. 8, pp. 974–978, Apr. 2009.
[21] I. S. Gradshteyn and I. M. Ryzhik, *Table of Integrals, Series, and Products,* 6th ed. San Diego, CA, USA: Academic, 2000.
[22] S. S. Ikki and M. H. Ahmed, "On the performance of cooperative-diversity networks with the Nth best-relay selection scheme," *IEEE Trans. Commun.*, vol. 58, no. 11, pp. 3062–3068, Nov. 2010.
[23] Y. Mao, J. Jin, and D. Zhang, "Throughput and channel access statistics of generalized selection multiuser scheduling," *IEEE Trans. Wireless Commun.*, vol. 7, no. 8, pp. 2975–2987, Aug. 2008.
[24] B. C. Arnold, N. Balakrishnan, and H. N. Nagaraja, *A First Course in Order Statistics*. New York, NY, USA: Wiley, 1992.
[25] M. Chiani, D. Dardari, and M. K. Simon, "New exponential bounds and approximations for the computation of error probability in fading channels," *IEEE Trans. Wireless Commun.*, vol. 2, no. 4, pp. 840–845, Jul. 2003.
[26] Y. Zhao, R. Adve, and T. J. Lim, "Symbol error rate of selection amplify-and-forward relay systems," *IEEE Commun. Lett.*, vol. 10, no. 11, pp. 757–759, Nov. 2006.
[27] M.-S. Alouini and A. J. Goldsmith, "Capacity of Rayleigh fading channels under different adaptive transmission and diversity-combining techniques," *IEEE Trans. Veh. Technol.*, vol. 48, no. 4, pp. 1165–1181, Jul. 1999.
[28] L. Zheng and D. N. C. Tse, "Diversity and multiplexing: A fundamental tradeoff in multiple antenna channels," *IEEE Trans. Inf. Theory*, vol. 49, no. 5, pp. 1073–1096, May 2003.
[29] C.-J. Chen and L.-C. Wang, "Enhancing coverage and capacity for multiuser MIMO systems by utilizing scheduling," *IEEE Trans. Wireless Commun.*, vol. 5, no. 5, pp. 1148–1157, May 2006.
[30] A. K. Majumdar, "Free-space laser communication performance in the atmospheric channel," *J. Opt. Fiber Commun. Rep.*, vol. 2, no. 4, pp. 345–396, Oct. 2005.